

Generating mesoscopic Bell states via collisions of distinguishable quantum bright solitons

Bettina Gertjerenken,¹ Thomas P. Billam,² Caroline L. Blackley,³ C. Ruth Le Sueur,³ Lev Khaykovich,⁴ Simon L. Cornish,⁵ and Christoph Weiss^{5,*}

¹*Institut für Physik, Carl von Ossietzky Universität, D-26111 Oldenburg, Germany*

²*Jack Dodd Center for Quantum Technology, Department of Physics, University of Otago, Dunedin 9016, New Zealand*

³*Joint Quantum Centre (JQC) Durham–Newcastle, Department of Chemistry, Durham University, Durham DH1 3LE, United Kingdom*

⁴*Department of Physics, Bar-Ilan University, Ramat-Gan, 52900 Israel*

⁵*Joint Quantum Centre (JQC) Durham–Newcastle, Department of Physics, Durham University, Durham DH1 3LE, United Kingdom*

(Dated: August 27, 2013)

We investigate numerically the collisions of two distinguishable quantum matter-wave bright solitons in a one-dimensional harmonic trap. We show that such collisions can be used to generate mesoscopic Bell states which can reliably be distinguished from statistical mixtures. Calculation of the relevant s-wave scattering lengths predicts that such states could potentially be realized in quantum-degenerate mixtures of ⁸⁵Rb and ¹³³Cs. In addition to fully quantum simulations for two distinguishable two-particle solitons, we use a mean-field description supplemented by a stochastic treatment of quantum fluctuations in the soliton's center of mass: We demonstrate the validity of this approach by comparison to a mathematically rigorous effective potential treatment of the quantum many-particle problem.

PACS numbers: 03.75.Gg, 03.75.Lm, 03.75.Mn, 67.85.-d,

Keywords: Bell state, matter-wave soliton, bright soliton, effective potential method, classical field method

Generating quantum entanglement between mesoscopic objects over mesoscopic distances allows exploration of a fascinating “middle-ground” between quantum and classical physics [1, 2], and promises significant advances in quantum-enhanced interferometry [3]. The high degree of experimental control offered by quantum-degenerate gases makes them an ideal platform with which to explore such multi-particle entanglement [4, 5]. From a fundamental perspective, the creation of *maximally-entangled* many-particle Bell states in quantum-degenerate gases presents an intriguing proposition. The generation of similar macroscopic Bell states of many photons is an area of current theoretical and experimental research [6, 7]. In addition to their inherent fundamental interest, such states are of potential application as a resource in quantum information [7].

Previously, the scattering of quantum bright matter-wave solitons [8–17] in quasi-one-dimensional (1D) trapping geometries has been suggested as a way to create mesoscopic entangled states in single-species Bose-Einstein condensates (BECs) [13, 18, 19]. In this Letter we consider a dual-species BEC [20, 21], and show that collisions of distinguishable quantum bright matter-wave solitons can be used to generate mesoscopic Bell states [22] (cf. [23]),

$$|\psi_{\text{Bell}}\rangle \equiv \frac{1}{\sqrt{2}} (|A, B\rangle + e^{i\alpha} |B, A\rangle), \quad (1)$$

where $|A, B\rangle$ ($|B, A\rangle$) signifies that the BEC A is on the left (right) and the BEC B is on the right (left). In particular, we show that a favorable combination of inter- and intra-species s-wave scattering lengths means that such states may be realized using ⁸⁵Rb and ¹³³Cs mixtures. We also show that the interference properties of these bright-soliton Bell states distinguish them from statistical mixtures. In contrast to the Bell ground states associated with double-well potentials, our collisionally-generated Bell states are robust to the presence of asymmetries. While distinguishable solitons are essential to produce Bell states, entanglement generation for solitons of the same species was investigated in [13].

For our quasi-1D system, we consider an experimentally motivated harmonic confinement $\omega = 2\pi f$. Mixtures of ultracold gases can be confined in a common optical trap with the same trap frequencies [24], yielding

$$\omega = \frac{2\pi}{T}; \quad \lambda_A = \sqrt{\frac{\hbar}{m_A \omega}}; \quad \lambda_B = \sqrt{\frac{\hbar}{m_B \omega}}, \quad (2)$$

where m_A (m_B) is the atomic mass of species A (B); the interactions $g = \hbar f_{\perp} a$ are set by the scattering lengths a and the perpendicular trapping-frequency, f_{\perp} [25].

* Christoph.Weiss@durham.ac.uk

We use the Lieb-Liniger model [26] for two species with

additional harmonic confinement

$$\begin{aligned} \hat{H} = & - \sum_{j=1}^{N_A} \frac{\hbar^2}{2m_A} \partial_{x_j}^2 + \sum_{j=1}^{N_A-1} \sum_{n=j+1}^{N_A} g_A \delta(x_j - x_n) \\ & - \sum_{j=1}^{N_B} \frac{\hbar^2}{2m_B} \partial_{y_j}^2 + \sum_{j=1}^{N_B-1} \sum_{n=j+1}^{N_B} g_B \delta(y_j - y_n) \\ & + \sum_{j=1}^{N_A} \sum_{n=1}^{N_B} g_{AB} \delta(x_j - y_n) \\ & + \sum_{j=1}^{N_A} \frac{1}{2} m_A \omega^2 x_j^2 + \sum_{j=1}^{N_B} \frac{1}{2} m_B \omega^2 y_j^2, \end{aligned} \quad (3)$$

where x_j (y_j) and $g_A < 0$ ($g_B < 0$) are the atomic coordinates and intra-species interactions of species A (B), and $g_{AB} \geq 0$ is the inter-species interaction.

We suggest to prepare the two solitons independently; for weak harmonic confinement a single soliton has the ground state energy (cf. [27])

$$E_S(N_S) = -\frac{1}{24} \frac{m_S g_S^2}{\hbar^2} N_S(N_S^2 - 1); \quad S \in \{A, B\}. \quad (4)$$

Thus, our system has the total ground-state energy

$$E_0 = E_A(N_A) + E_B(N_B). \quad (5)$$

The total kinetic energy related to the center-of-mass momenta $\hbar K_S$ ($S \in \{A, B\}$) of the two solitons reads

$$E_{\text{kin}} = \frac{\hbar^2 K_A^2}{2N_A m_A} + \frac{\hbar^2 K_B^2}{2N_B m_B}. \quad (6)$$

We extend the low-energy regime investigated for single-species solitons in Refs. [12, 18, 28] to two species:

$$E_{\text{kin}} < \min\{\Delta_A, \Delta_B\}, \quad \Delta_S = |E_S(N_S - 1) - E_S(N_S)|.$$

In this energy regime, each of the quantum matter-wave bright solitons is energetically forbidden to break up into two or more parts. Highly entangled states are characterized by a roughly 50:50 chance of finding the soliton A (B) on the left/right combined with a left/right correlation close to one indicating that whenever soliton A is on the one side, soliton B is on the other:

$$\begin{aligned} \gamma(\delta) \equiv & \int_{\delta}^{\infty} dx_1 \dots \int_{\delta}^{\infty} dx_{N_A} \int_{-\infty}^{-\delta} dy_1 \dots \int_{-\infty}^{-\delta} dy_{N_B} |\Psi|^2 \\ & + \int_{-\infty}^{-\delta} dx_1 \dots \int_{-\infty}^{-\delta} dx_{N_A} \int_{\delta}^{\infty} dy_1 \dots \int_{\delta}^{\infty} dy_{N_B} |\Psi|^2, \end{aligned} \quad (7)$$

where $\Psi = \Psi(x_1, \dots, x_{N_A}, y_1, \dots, y_{N_B})$ is the many-particle wave function (normalized to one) and $\delta \geq 0$. The correlation $\gamma(\delta)$ will serve as an indication of entanglement: Bell states (1) are characterized by $\gamma \simeq 1$ combined with a 50:50 chance to find soliton A either on one side or on the other.

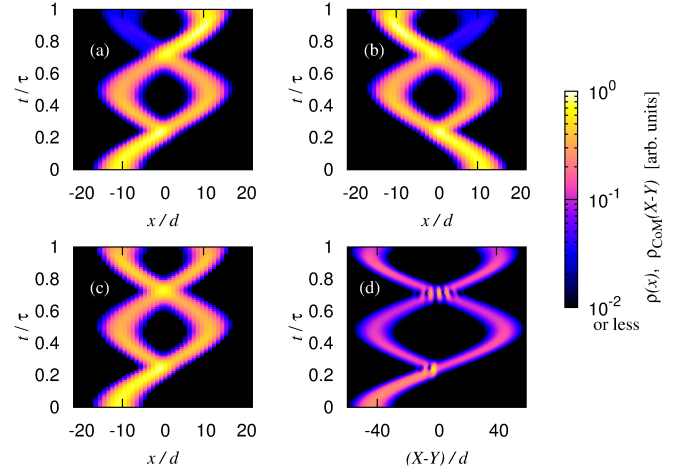


FIG. 1. (Color online) Collisions of two distinguishable dimers in the Bose-Hubbard Hamiltonian (8). (a) Single-particle density $\rho(x)$ of dimer A in a two-dimensional projection as a function of space and time (τ is the oscillation period without inter-species interaction, $U_A = -3J$, $U_B = -3J$, $U_{AB} = J$ and $C = 0.002J$). (b) Single-particle density of dimer B, parameters as in panel (a). (c) The same dimer as in panel (a) but the wave function is numerically turned into a statistical mixture at $t = \tau/2$. (d) Center-of-mass density $\rho_{\text{COM}}(X-Y)$ if the inter-species interaction is switched off at $t = \tau/2$, all other parameters as in (a) and (b). The interference pattern near $t = 0.7\tau$, combined with a high correlation (7) of $\gamma(d/2) \simeq 0.988$ near $t = 0.5\tau$, indicates that a Bell state has been created.

We begin by investigating entanglement-generating collisions of two distinguishable two-particle solitons (dimers). Discarding cases where the two solitons have distinct total masses $N_A m_A$ and $N_B m_B$ (small differences in the total masses would introduce small asymmetries without changing the physics), leads to $m_A = m_B = m$, which corresponds to having two hyperfine states of the same species. To describe the collisions of the two dimers, we discretize the Hamiltonian (3), yielding the Bose-Hubbard Hamiltonian (cf. [29])

$$\begin{aligned} \hat{H}_{\text{BH}} = & \sum_{\ell} \left\{ \frac{U_A}{2} \hat{a}_{\ell}^{\dagger} \hat{a}_{\ell}^{\dagger} \hat{a}_{\ell} \hat{a}_{\ell} + \frac{U_B}{2} \hat{b}_{\ell}^{\dagger} \hat{b}_{\ell}^{\dagger} \hat{b}_{\ell} \hat{b}_{\ell} + U_{AB} \hat{a}_{\ell}^{\dagger} \hat{a}_{\ell} \hat{b}_{\ell}^{\dagger} \hat{b}_{\ell} \right. \\ & - J \left(\hat{a}_{\ell}^{\dagger} \hat{a}_{\ell+1} + \hat{a}_{\ell+1}^{\dagger} \hat{a}_{\ell} + \hat{b}_{\ell}^{\dagger} \hat{b}_{\ell+1} + \hat{b}_{\ell+1}^{\dagger} \hat{b}_{\ell} \right) \\ & \left. + C \ell^2 \hat{a}_{\ell}^{\dagger} \hat{a}_{\ell} + C \ell^2 \hat{b}_{\ell}^{\dagger} \hat{b}_{\ell} \right\}, \end{aligned} \quad (8)$$

where U_A , U_B and U_{AB} are the intra-species and inter-species interactions, the hopping is given by $J \sim \hbar^2/(2md^2)$ for grid spacing $d \rightarrow 0$ and $C \equiv 0.5m\omega^2 d^2$.

Figure 1 shows two-dimensional projections of the dynamics of two distinguishable dimers. The two dimers were numerically prepared in the ground state of two spatially separated harmonic oscillators via imaginary time-evolution [30]. At time $t = 0$ they were transferred into the same harmonic oscillator potential (without overlap). Subsequently, the time-evolution was calculated

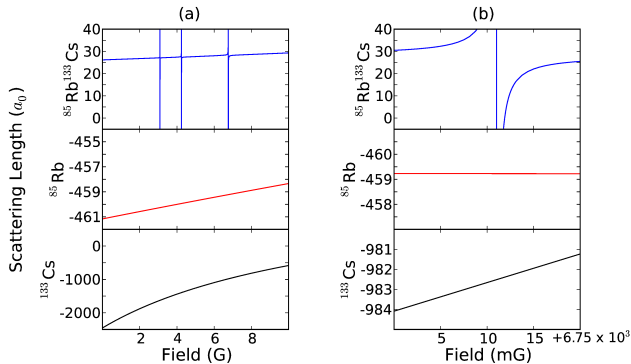


FIG. 2. (Color online) The s-wave scattering lengths for the ground state of $^{85}\text{Rb}^{133}\text{Cs}$, ^{85}Rb and ^{133}Cs respectively. **(a)** Scattering lengths are calculated using a coupled-channels method [21] with a fully decoupled basis set at a collision energy of 1 pK. The calculations are performed using the MOLSCAT program [33] adapted to handle collisions in external fields [34]. The RbCs potential is from [21], Rb from [35] and Cs from [36]. Resonances for $^{85}\text{Rb}^{133}\text{Cs}$ are at 3.10 G, 4.27 G and 6.76 G [37]. **(b)** Zoom of (a).

using the full Schrödinger equation corresponding to the Hamiltonian (8). After the first collision, a measurement would reveal dimer A on the left and dimer B on the right or vice versa [the correlation (7) is $\gamma(d/2) \simeq 0.988$].

As the sizes of the dimers in panels Fig. 1 (a) and (b) are not too large compared to the oscillator length, after the second collision both dimers are more likely to be on the side opposite to their initial condition than at the same side (cf. the single soliton case [28]). This can be used to distinguish a pure quantum superposition from a statistical mixture [Fig. 1 (c)]. A more general approach extends the center-of-mass density [31] to two solitons [Fig. 1 (d)]: After switching off the inter-species interaction when the Bell-state has formed, one first measures the center of mass X and Y of solitons A and B and then plots the resulting density ϱ_{CoM} as a function of the difference $X - Y$. This works both for superpositions of plane waves $\exp[iKX] \exp[-iKY] + \exp[-iKX] \exp[iKY]$ with

$$\varrho_{\text{CoM}}(X - Y) \propto \{\cos[K(X - Y)]\}^2 \quad (9)$$

and when the two wave packets recombine [Fig. 1 (d)]. Measuring a contrast close to one as in Eq. (9) is possible as the center of mass can be measured with higher accuracy than the soliton width (cf. [31]). As shown in Ref. [31] for the single-species case, CoM interferences do, in general, not correspond to interferences in single-particle densities which have been investigated, e.g., for distinguishable BECs in Ref. [32].

To show that attractive intra-species interactions and repulsive, *tunable* inter-species interactions are experimentally feasible, we calculate the s-wave scattering lengths for $^{85}\text{Rb}^{133}\text{Cs}$. The results displayed in Fig. 2 shows a candidate inter-species Feshbach resonance at

6.76 G suitable for our requirements [37]. For lower magnetic fields the magnetic field can be stabilized to up to 100 μG [38]; shielding allows stabilization to 1 mG below 10 G. Although the masses of the atoms A and B now differ, we can still have two solitons of roughly the same total masses $N_A m_A$ and $N_B m_B$ as in Fig. 1.

Behavior for larger particle numbers can be described by the Gross-Pitaevskii equation (GPE) (cf. [39–42])

$$\begin{aligned} i\hbar\partial_t\varphi_A(x,t) &= \left[-\frac{\hbar^2}{2m_A}\partial_x^2 + \frac{g_A}{2}|\varphi_A(x,t)|^2 \right] \varphi_A(x,t) \\ &\quad + \left[\frac{1}{2}m_A\omega^2x^2 + \frac{g_{AB}}{2}|\varphi_B(x,t)|^2 \right] \varphi_A(x,t) \\ i\hbar\partial_t\varphi_B(x,t) &= \left[-\frac{\hbar^2}{2m_B}\partial_x^2 + \frac{g_B}{2}|\varphi_B(x,t)|^2 \right] \varphi_B(x,t) \\ &\quad + \left[\frac{1}{2}m_B\omega^2x^2 + \frac{g_{AB}}{2}|\varphi_A(x,t)|^2 \right] \varphi_B(x,t), \end{aligned}$$

where the single-particle density $|\varphi_S(x,t)|^2$ is normalized to N_S ($S \in \{A, B\}$).

When hitting a barrier, the generic behavior of a mean-field bright soliton is to break into two parts; the fraction of the atoms transmitted decreases for increasing potential strength (cf. [15, 17]). An analogous behavior also occurs when two mean-field bright solitons hit each other as shown in the Supplemental Material [43].

Low kinetic energies generate very different GPE dynamics. For the case of a single-species soliton incident upon a potential barrier one observes a sharp stepwise jump in the GPE reflection coefficient as a function of barrier height [16, 28, 44]. In this case we previously [28] showed that this jump occurs in regimes where, on the N -particle quantum level, the low kinetic energies prevent the soliton from breaking into two (or more) smaller solitons, and thus provides a useful GPE-level indicator for the formation of N -particle quantum superpositions.

Conjecturing that sharp stepwise jumps in the GPE reflection coefficient for distinguishable soliton collisions may indicate Bell states, we investigate parameters yielding such jumps (cf. Supplemental Material [43]). To confirm that these jumps indicate Bell state formation, we use the truncated-Wigner approximation (TWA), which describes quantum systems by averaging over realizations of an appropriate classical field equation (in this case, the GPE) with initial noise appropriate to either finite [45] or zero temperatures [15]. While the GPE assumes both position and momentum are well defined, this is not true for a single quantum particle of finite mass for which, in general, both position and momentum involve quantum noise satisfying the uncertainty relation. Our TWA calculations for the soliton center-of-mass wave function use Gaussian probability distributions for both (satisfying minimal uncertainty).

In order to demonstrate that the center-of-mass TWA is indeed a valid approach to describe the short-time behavior of mesoscopic quantum superpositions, Fig. 3 starts with the case where a light soliton hits a

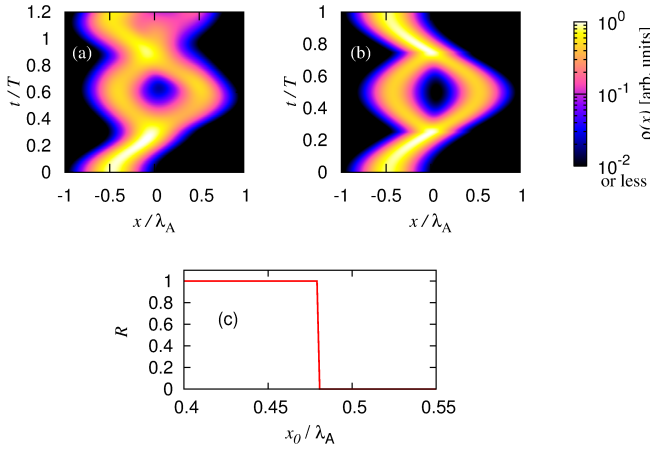


FIG. 3. (Color online) (a) Single-particle density for an N -particle quantum bright soliton hitting a narrow, heavy non-moving soliton, computed using the effective potential approach (footnote 1). (b) As in (a) but using the TWA for the center of mass. The parameters are in the low kinetic energy regime such that the GPE predicts a sharp stepwise [28] behavior of reflection coefficient as a function of the initial displacement shown in panel (c); $U_0 \simeq 12\hbar\omega$ (cf. footnote 1).

heavy, non-moving soliton. In panel (a), the rigorously proved [46] effective potential approach [12, 18]¹ demonstrates the emergence of a Schrödinger-cat state when the GPE predicts the stepwise behavior of the reflection coefficient explained in Refs. [16, 28, 44] [Fig. 3 (c)].

In panel (b), we use the TWA to average over the analytic approximation for the classical-particle-like behavior of the GPE-soliton [47]. This leads to a good qualitative agreement with the N -particle predictions in panel (a) up to the time where both parts of the wave function recombine and quantum interference becomes important.

On the N -particle level, the low kinetic energies are important for the soliton not to be able to break into two (or more) smaller solitons. While GPE-solitons can, during a collision, lose a small fraction of particles, for low kinetic energies this effect becomes negligible [24]. Thus, the sharp stepwise behavior shown in Fig. 3 (c) leads to a behavior very close to the true N -particle quantum case.

In order to observe Bell states, we investigate two distinguishable bright solitons of similar mass at low kinetic energy ($E_{\text{kin}}/|E_0| = 0.182$). Applying the TWA for the center-of-mass wave functions of both solitons leads to

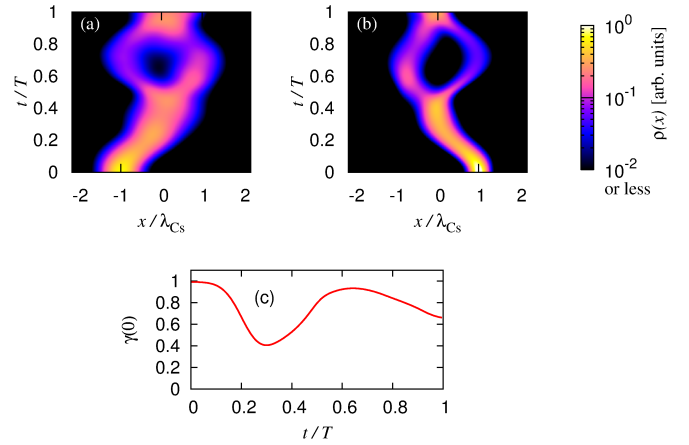


FIG. 4. (Color online) TWA for the center of mass in the low-kinetic-energy regime applied to the two-species GPE. The single particle density for the ^{133}Cs -soliton is displayed in panel (a), for ^{85}Rb in panel (b). (c) This leads to a correlation (7) close to one, thus indicating a Bell state. Parameters: $a_{Cs} = -982.5a_0$, $a_{Rb} = -459.2a_0$, $f = 1\text{Hz}$, $f_{\perp} = 70\text{Hz}$, $N_{Cs} \simeq 12$, $N_{Rb} \simeq 19$ (corresponding to $N_{Rb}m_{Rb} \approx N_{Cs}m_{Cs}$, thus avoiding center-of-mass movement), $a_{RbCs} = 63.6a_0$, and the initial displacement from trap center: $-8.7\mu\text{m}$ for ^{133}Cs and $+8.7\mu\text{m}$ for ^{85}Rb .

the single-particle densities displayed in Fig. 4 (a) and (b). The low kinetic energies indicate that the feature shown in those single-particle densities near $t \approx 0.6T$ should indeed be a Bell state. The value of the correlation function close to one [Fig. 4 (c)] shows that we indeed have found a Bell state. While the TWA is no longer valid as soon as both parts of the wave-function overlap, a full quantum mechanical calculation would also lead to a decrease of the correlation in Fig. 4 (c) on this time-scale.

To conclude, based on predictions made on the level of many-particle quantum calculations (using the Lieb-Liniger model), we demonstrated numerically that mesoscopic Bell states can be generated by colliding two distinguishable quantum matter-wave bright solitons. In experiment, the formation of these states could be confirmed by switching off the inter-species interaction once the Bell state has formed and then measuring the interference fringes in the combined center-of-mass density (9) [see Fig. 1], revealing the presence of quantum superposition. Finally, we have shown that matter-wave bright solitons in ^{85}Rb - ^{133}Cs mixtures are a promising candidate system for experimental realization of mesoscopic Bell states, presenting an intriguing target for future experimental investigations.

ACKNOWLEDGMENTS

We thank C. S. Adams, S. A. Gardiner, J. L. Helm, J. M. Hutson and M. P. Köppinger for discussions. We

¹ This approach replaces the N -particle Schrödinger equation by a single-particle Schrödinger equation for the center-of-mass coordinate. The effective potential is the convolution of the soliton with the potential seen by single particles [12, 18], in our case the soliton B which is chosen to be a factor of $N_{BgB}/(N_A g_A) = 10$ narrower than soliton A: $U_1[\cosh(N_{BgB}x)]^{-2} \simeq 2U_1/(N_{BgB})\delta(x)$. If soliton A hits the narrow soliton B [Fig. 3 (a)], the effective potential $U_0[\cosh(N_A g_A x)]^{-2}$ has the GPE-shape of the A-soliton with $U_0 = N_A U_1 N_A g_A / (N_{BgB}) = 10U_1$, for $N_A = 100$.

thank the *Studienstiftung des deutschen Volkes* (B.G.), the *Heinz Neumüller Stiftung* (B.G.), the Marsden Fund of New Zealand (contract UOO162) and the Royal Society of New Zealand (contract UOO004) (T.P.B.), the Faculty of Science at Durham University (C.L.B.), the EOARD (Grant FA8655-10-1-3033, C.R.LS) and the UK EPSRC (Grant No. EP/G05 6781/1, C.W.) for funding.

Appendix A: Supplemental Material: Collision behavior of higher-kinetic-energy Gross-Pitaevskii bright solitons

The mean-field approach via the Gross-Pitaevskii equation (GPE) [48] provides physical insight into the behavior of bright solitons:

$$i\hbar\partial_t\varphi(x,t) = -\frac{\hbar^2}{2m}\partial_x^2\varphi(x,t) + V_{\text{ext}}(x)\varphi(x,t) + (N-1)g_{1D}|\varphi(x,t)|^2\varphi(x,t),$$

where m is the mass of one atom, N is the number of atoms, $V_{\text{ext}}(x)$ is the external potential and g_{1D} quantifies the (contact-)interaction between two particles; the single-particle density $|\varphi(x,t)|^2$ is normalized to one. Without a scattering potential [$V_{\text{ext}}(x) = 0$], exact solutions for GPE-solitons exist [48]

$$\varphi(x,0) = \sqrt{\frac{2\mu}{(N-1)g_{1D}}} \frac{e^{im\mu x/\hbar - i(\mu - mu^2/2)t/\hbar}}{\cosh\left[\sqrt{\frac{2m|\mu|}{\hbar^2}}(x - x_0 - ut)\right]},$$

here u is the velocity and x_0 the initial position; normalizing $|\varphi(x,0)|^2$ to one yields (cf. [49])

$$\mu = -\frac{1}{8} \frac{mg_{1D}^2}{\hbar^2} (N-1)^2.$$

In the regime of high kinetic energies [28, 50],

$$E_{\text{kin}} \gg E_0,$$

where

$$E_{\text{kin}} = N\hbar^2 k^2 / (2m)$$

and

$$E_0 = -mg_{1D}^2 N(N^2 - 1) / (24\hbar^2),$$

scattering a soliton from a narrow barrier behaves essentially like scattering a single particle of such a barrier. For high enough kinetic energies, a bright soliton scattering off a delta-function barrier has the same transmission/reflection behavior [50] as the textbook example of a single particle scattered off such a potential [51].

There is, however, an important difference between the single particle case and high-energy bright solitons: For single particles, such a transmission/reflection behavior can only be measured by repeating the experiment often

(the particle will always be measured either on one side or on the other side of the delta-function barrier). For a bright soliton, a transmission larger than 0 and lower than one leads to a (in an ideal experiment reproducible) fraction of the atoms being found on either side in *each single experiment*.

In order to show that this “classical” breaking-into-two-parts behavior also occurs for two collisions of two high-energy distinguishable bright solitons, we use the GPE (cf. [39–42])

$$\begin{aligned} i\hbar\partial_t\varphi_A(x,t) &= \left[-\frac{\hbar^2}{2m_A}\partial_x^2 + \frac{g_A}{2}|\varphi_A(x,t)|^2 \right] \varphi_A(x,t) \\ &\quad + \left[\frac{1}{2}m_A\omega^2 x^2 + \frac{g_{AB}}{2}|\varphi_B(x,t)|^2 \right] \varphi_A(x,t) \\ i\hbar\partial_t\varphi_B(x,t) &= \left[-\frac{\hbar^2}{2m_B}\partial_x^2 + \frac{g_B}{2}|\varphi_B(x,t)|^2 \right] \varphi_B(x,t) \\ &\quad + \left[\frac{1}{2}m_B\omega^2 x^2 + \frac{g_{AB}}{2}|\varphi_A(x,t)|^2 \right] \varphi_B(x,t), \end{aligned}$$

where the single-particle density $|\varphi_S(x,t)|^2$ is normalized to N_S ($S \in \{A, B\}$), $g_A < 0$ ($g_B < 0$) the intra-species interactions of species A (B), and $g_{AB} \geq 0$ is the inter-species interaction.

Figure 5 shows typical GPE dynamics in the regime where the kinetic energy E_{kin} is large compared to the ground state energy $|E_0|$ ($E_{\text{kin}}/|E_0| = 84.9$). Here, both solitons split such that close to 50% of the particles of each species are on each side of the center of the trap for times near $t = T/2$, and the correlation function

$$\begin{aligned} \gamma(\delta) &\equiv \int_{\delta}^{\infty} dx_1 \dots \int_{\delta}^{\infty} dx_{N_A} \int_{-\infty}^{-\delta} dy_1 \dots \int_{-\infty}^{-\delta} dy_{N_B} |\Psi|^2 \\ &\quad + \int_{-\infty}^{-\delta} dx_1 \dots \int_{-\infty}^{-\delta} dx_{N_A} \int_{\delta}^{\infty} dy_1 \dots \int_{\delta}^{\infty} dy_{N_B} |\Psi|^2, \end{aligned} \quad (\text{A1})$$

depicted in Fig. 5 (c) shows no signs of Bell states (which would lead to correlations close to one).

We extend the exact lower bounds on the reflection coefficient R for a single soliton scattered off a barrier [28] to the case of two distinguishable solitons [Fig. 5 (d) and (e)], where

$$R_{\text{min}} \equiv \min\{R \geq 0.5\}. \quad (\text{A2})$$

Panels (d) and (e) of Fig. 5 show that using roughly equal total masses $N_A m_A$ and $N_B m_B$, $N_{\text{Rb}} \approx 1.6 N_{\text{Cs}}$ is indeed a good idea for entanglement generation: at approximately this ratio do jumps occur in both reflection coefficients for kinetic energies corresponding to reasonable timescales (without a trap) or initial displacements (in the presence of a trap).

Only by focusing on low kinetic energies, two distinguishable bright solitons (of equal soliton mass) would start to behave similar to large molecules: after a collision all atoms of one kind would be measured either be

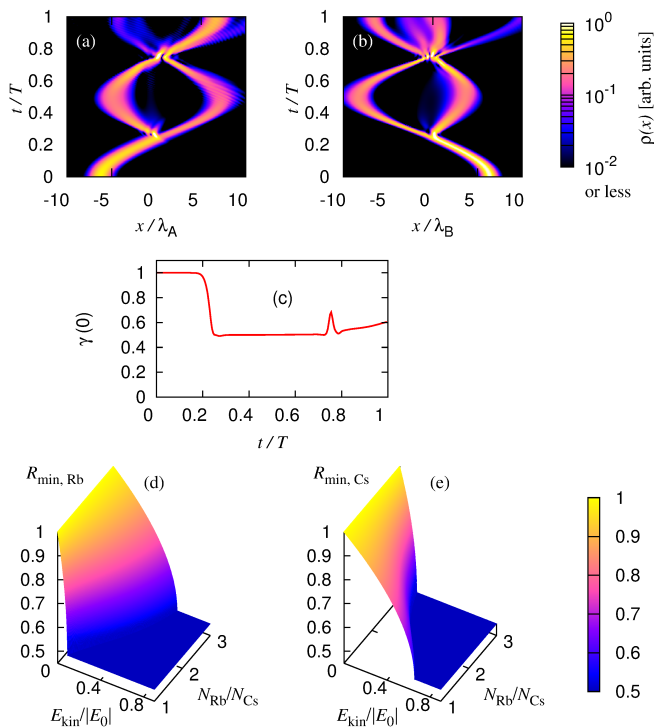


FIG. 5. (a) Single-particle density for a GPE-soliton of ^{133}Cs atoms splits at high kinetic energies when hitting the soliton made of ^{85}Rb atoms. Parameters are the s -wave scattering lengths $a_{\text{Cs}} = -982.5a_0$, $a_{\text{Rb}} = -459.2a_0$, $a_{\text{RbCs}} = 8351a_0$, axial frequency $f = 1\text{Hz}$ and radial frequency $f_{\perp} = 16\text{Hz}$, as well as particle numbers $N_{\text{Cs}} \simeq 17$, $N_{\text{Rb}} \simeq 17$. The starting displacement from the trap center: $\pm 55.2\mu\text{m}$ (b) Single-particle density for the soliton made of ^{85}Rb atoms for the simulation depicted in panel (a). (c) Although the single-particle densities of panels (a) and (b) look similar to what Bell-state would look like, at $t \approx T/2$ we have a low correlation (A1) and therefore no Bell state. (d) and (e) show lower bounds on R_{\min} [Eq. (A2) cf. [28]].

on one side or on the other of the center of mass. Such cases are relevant for entanglement generation, and form the subject of the main paper.

-
- [1] L. Hackermuller, K. Hornberger, B. Brezger, A. Zeilinger, and M. Arndt, *Nature (London)* **427**, 711 (2004)
 - [2] W. H. Zurek, *Rev. Mod. Phys.* **75**, 715 (2003)
 - [3] V. Giovannetti, S. Lloyd, and L. Maccone, *Science* **306**, 1330 (2004)
 - [4] J. Estève, C. Gross, A. Weller, S. Giovanazzi, and M. K. Oberthaler, *Nature* **455**, 1216 (2008)
 - [5] M. F. Riedel, P. Böhi, Y. Li, T. W. Hänsch, A. Sinatra, and P. Treutlein, *Nature* **464**, 1170 (2010)
 - [6] M. Stobińska, F. Töppel, P. Sekatski, and M. V. Chekhova, *Phys. Rev. A* **86**, 022323 (2012)
 - [7] T. S. Iskhakov, I. N. Agafonov, M. V. Chekhova, and G. Leuchs, *Phys. Rev. Lett.* **109**, 150502 (2012)
 - [8] L. Khaykovich, F. Schreck, G. Ferrari, T. Bourdel, J. Cubizolles, L. D. Carr, Y. Castin, and C. Salomon, *Science* **296**, 1290 (2002)
 - [9] K. E. Strecker, G. B. Partridge, A. G. Truscott, and R. G. Hulet, *Nature (London)* **417**, 150 (2002)
 - [10] H. Buljan, M. Segev, and A. Vardi, *Phys. Rev. Lett.* **95**, 180401 (2005)
 - [11] S. L. Cornish, S. T. Thompson, and C. E. Wieman, *Phys. Rev. Lett.* **96**, 170401 (2006)
 - [12] K. Sacha, C. A. Müller, D. Delande, and J. Zakrzewski, *Phys. Rev. Lett.* **103**, 210402 (2009)
 - [13] M. Lewenstein and B. A. Malomed, *New J. Phys.* **11**, 113014 (2009)
 - [14] T. Ernst and J. Brand, *Phys. Rev. A* **81**, 033614 (2010)
 - [15] A. D. Martin and J. Ruostekoski, *New J. Phys.* **14**, 043040 (2012)
 - [16] S. Damgaard Hansen, N. Nygaard, and K. Mølmer, *ArXiv e-prints(2012)*, arXiv:1210.1681
 - [17] J. Cuevas, P. G. Kevrekidis, B. A. Malomed, P. Dyke, and R. G. Hulet, *New Journal of Physics* **15**, 063006 (2013)
 - [18] C. Weiss and Y. Castin, *Phys. Rev. Lett.* **102**, 010403 (2009)
 - [19] A. I. Streltsov, O. E. Alon, and L. S. Cederbaum, *Phys. Rev. A* **80**, 043616 (2009)

- [20] D. J. McCarron, H. W. Cho, D. L. Jenkin, M. P. Köppinger, and S. L. Cornish, *Phys. Rev. A* **84**, 011603 (2011)
- [21] T. Takekoshi, M. Debatin, R. Rameshan, F. Ferlaino, R. Grimm, H.-C. Nägerl, C. R. Le Sueur, J. M. Hutson, P. S. Julienne, S. Kotochigova, and E. Tiemann, *Phys. Rev. A* **85**, 032506 (2012)
- [22] G. Csire and B. Apagyi, *Phys. Rev. A* **85**, 033613 (2012)
- [23] M. A. Garcia-March, D. R. Dounas-Frazer, and L. D. Carr, *Phys. Rev. A* **83**, 043612 (2011)
- [24] M. S. Safronova, B. Arora, and C. W. Clark, *Phys. Rev. A* **73**, 022505 (2006)
- [25] M. Olshanii, *Phys. Rev. Lett.* **81**, 938 (1998)
- [26] E. H. Lieb and W. Liniger, *Phys. Rev.* **130**, 1605 (1963)
- [27] J. B. McGuire, *J. Math. Phys.* **5**, 622 (1964)
- [28] B. Gertjerenken, T. P. Billam, L. Khaykovich, and C. Weiss, *Phys. Rev. A* **86**, 033608 (2012)
- [29] E. Altman, W. Hofstetter, E. Demler, and M. D. Lukin, *New J. Phys.* **5**, 113 (2003)
- [30] J. A. Glick and L. D. Carr, *ArXiv e-prints*(2011), arXiv:1105.5164
- [31] B. Gertjerenken and C. Weiss, *J. Phys. B* **45**, 165301 (2012)
- [32] L. S. Cederbaum, A. I. Streltsov, Y. B. Band, and O. E. Alon, *Phys. Rev. Lett.* **98**, 110405 (2007)
- [33] J. M. Hutson and S. Green, “MOLSCAT computer program, version 14,” distributed by Collaborative Computational Project No. 6 of the UK Engineering and Physical Sciences Research Council (1994)
- [34] M. L. González-Martínez and J. M. Hutson, *Phys. Rev. A* **75**, 022702 (2007)
- [35] C. Strauss, T. Takekoshi, F. Lang, K. Winkler, R. Grimm, J. Hecker Denschlag, and E. Tiemann, *Phys. Rev. A* **82**, 052514 (2010)
- [36] M. Berninger, A. Zenesini, B. Huang, W. Harm, H.-C. Nägerl, F. Ferlaino, R. Grimm, P. S. Julienne, and J. M. Hutson, *Phys. Rev. Lett.* **107**, 120401 (2011)
- [37] H.-W. Cho, D. J. McCarron, M. P. Köppinger, D. L. Jenkin, K. L. Butler, P. S. Julienne, C. L. Blackley, C. R. Le Sueur, J. M. Hutson, and S. L. Cornish, *Phys. Rev. A* **87**, 010703(R) (2013)
- [38] B. Pasquiou, E. Maréchal, L. Vernac, O. Gorceix, and B. Laburthe-Tolra, *Phys. Rev. Lett.* **108**, 045307 (2012)
- [39] H. Pu and N. P. Bigelow, *Phys. Rev. Lett.* **80**, 1134 (1998)
- [40] E. Timmermans, *Phys. Rev. Lett.* **81**, 5718 (1998)
- [41] P. Öhberg and L. Santos, *Phys. Rev. Lett.* **86**, 2918 (2001)
- [42] He, Z.M., Wang, D.L., Ding, J.W., and Yan, X.H., *Eur. Phys. J. D* **66**, 139 (2012)
- [43] See Supplemental Material in the appendix to see that bright solitons break apart during collisions at higher kinetic energies and only behave similar to a big molecule for low kinetic energies.
- [44] C.-H. Wang, T.-M. Hong, R.-K. Lee, and D.-W. Wang, *Opt. Express* **20**, 22675 (2012)
- [45] P. Bienias, K. Pawłowski, M. Gajda, and K. Rzazewski, *EPL (Europhys. Lett.)* **96**, 10011 (2011)
- [46] C. Weiss and Y. Castin, *J. Phys. A* **45**, 455306 (2012)
- [47] A. D. Martin, C. S. Adams, and S. A. Gardiner, *Phys. Rev. A* **77**, 013620 (2008)
- [48] C. J. Pethick and H. Smith, *Bose-Einstein Condensation in Dilute Gases* (Cambridge University Press, Cambridge, 2008)
- [49] Y. Castin and C. Herzog, *C. R. Acad. Sci. Paris, Ser. IV* **2**, 419 (2001), arXiv:cond-mat/0012040
- [50] J. Holmer, J. Marzuola, and M. Zworski, *Commun. Math. Phys.* **274**, 187 (2007)
- [51] S. Flügge, *Rechenmethoden der Quantentheorie* (Springer, Berlin, 1990)